Original Research Article

Evaluation of Shielding effectiveness of Tellurite glass with composition 85TeO2-5Nb2O5-5ZnO-5Ag_2O for diagnostic radiology application [b]

1. Abstract

The metal oxide glasses have attracted huge interest as promising types of shielding materials to replace the toxic, heavy and costly conventional shielding materials. In this work, the physical and the shielding effectiveness of Tellurite glass sample contain host metal oxides (**85TeO_2-5Nb_2O_5-5ZnO-5Ag_2O**) were evaluated at photon energies range between 15keV and 1MeV. The shielding parameters of the proposed glass system such as linear attenuation coefficients, HVL, MFP, Z_{eff}, and N_{eff} were evaluated. The proposed samples showed a superior performance at the diagnostic energy range between 40 and 90 keV and a comparable shielding effectiveness above 90keV when compared with other commercial standard shielding materials.

Keywords: Tellurite glasses, Mass attenuation coefficient, Linear attenuation coefficient, Half-value layer, mean free path, Radiation shielding.

2. Introduction

Since the discovery of x-ray by Roentgen in 1895 and the radioactivity by Henri Becquerel in 1896, the radiation applications such as nuclear power, medical imaging, cancer treatment and nuclear engineering are dramatically increased over the past decades [1-3]. The improper use of radiation can lead to serious injuries. The severity of radiation injuries depends on the radiation exposure dose rate. The radiation risk and injuries in different application were widely addressed by several researcher [4-8].

The use of ionizing radiation required safety standards to be establish and implement to ensure the protection of people and environment, many standards for radiation protection and safety were stablished [9-12]. Exposure time, distance from the source and shielding are the basic principles of protection considered when dealing with ionizing radiation. Shielding is most important consideration for any facility that preform diagnostic or therapy procedures. Many factors affecting the effectiveness of a shielding materials used to protect people working in radiation facilities such radiation energy, radiation type, the thickness of shielding material. The denser the material the more effective shielding materials against X-rays and gamma rays. Lead is the most common material use in most of radiation applications as shielding material due to its high atomic number. Although, lead is the most effective material in attenuating gamma and X-ray photons but can cause pollution through release of lead particles and can affected all the system body [13-15].

Due to the toxicity, high cost, and heavy weight of lead and lead glass materials several studies were conducted to develop alternative materials that replace lead such as tellurite-base glasses, phosphate-based materials, metal alloy, polymers [16-40]. These studies showed a good shielding performance in terms of high shielding efficiency without loss of transparency, good physical properties, thermal stability and good optical properties.

The shielding effectiveness have been studies in terms of the physical properties, radiation shielding parameters, LAC, MAC, HVL, MFP , Z_{eff} and N_{eff}. Al-Hadeethi et.al [21] have studied the x-ray photons attenuation characteristics for two glass-based systems (Bi_2O_3 -B_2O_3 -TeO_2 – TiO_3 and PbO-ZnO-TeO_2-B_2O_3) at photon energies ranging from 30 to 80kVp. Their results showed that the increase of Tellurium dioxide (TeO_2) concentration increases the attenuation

coefficients of the glasses system with a decrease in the half-value layer especially at photon energy range between 70 and 80keV. Mhared et.al [22] have studied the shielding effectiveness of lithium-magnesium-borate glasses with Thulium oxide (Tm_2O_3). Their results showed that the attenuation coefficients increase with increasing Tm_2O_3 concentration. Lakshminarayana et.al [23] have studied the radiation shielding effectiveness of borosilicate glasses doped Tm^{3+} ions for gamma application. Their results indicates that the sample contain highest mole concentration of Tm_2O_3 has the greater ability to attenuate gamma-rays.

In this work, the shielding effectiveness of Tellurite based-glass system was investigated at photon energy range between 15keV and 1MeV. The radiation shielding parameters of the prepared glass system such as LAC, MAC, HVL, Z_{eff}, Z_{eq}, MFP, N_{eff} and EBF were calculated using the online developed software (Phy-X/PSD) [24]. The results of shielding parameters were compared with other commercial shielding materials commonly used in photon applications.

3. Theory and Method

Tellurite glasses samples contain different oxides ($85TeO_2$-$5Nb_2O_5$-$5ZnO$-$5Ag_2O$) were prepared by putting the raw material in Platinum crucible in the heating furnace at a temperature in range from 850 to 950 °C for 30 min. The melting material was stirred to increase the viscosity before cast in the brass mold. The prepared sample was put in the annealing furnace for 2h at 320 °C. The sample density was measured using *Archimedes*' Principle. Table 1 shows the density, molar weight (M_W) and the chemical compositions of the prepared sample.

Table 1. The Physical parameters and chemical compositions of the proposed glass sample

Sample code	**Mw (g/mol)**	**Density (g/cm^3) ± 0.04**	**Composition (mol%)**			
			TeO_2	**Nb_2O_5**	**ZnO**	Ag_2O
S1	164.61	5.3744	85	5	5	5

The average molar weight of mixtures $\bar{M}$ can be calculated using mole by fractions x_i and molar masses M_i of the constituent elements of the component and their [25]:

$$\bar{M} = \sum x_i M_{i,} \quad \textbf{(1)}$$

where x_i is the molar fraction of each component i, M_i is the molecular weight of the sample

The effectiveness of a shielding material can be investigated by the physical properties and radiation shielding parameters. The MAN, LAC, Z_{eff}, N_{eff}, HVL and MFP are the most important radiation shielding parameters that characterizing the effectiveness of the shielding materials. The cross section for scattering and absorption can be express in term of the total mass attenuation coefficient (μ/ρ), which can be calculated using the program Xcom [26]. The mass attenuation coefficient of a compound can be computed using the following relation [26-30]:

$$\frac{\mu}{\rho} = \sum_i w_i \left(\frac{\mu}{\rho}\right)_i \quad \textbf{(2)}$$

Where w_i is the fraction by weight of the ith atomic element and $\left(\frac{\mu}{\rho}\right)_i$ is the mass attenuation of the of the ith atomic element.

The probability of photon interaction with material can be characterized by the total atom cross-section (σ_a) and total electronic cross-section (σ_a) using the following relations [29-30]:

$$\sigma_a = \frac{1}{N_A} \sum_i f_i A_i \left(\frac{\mu}{\rho}\right)_i \quad \textbf{(3)}$$

$$\sigma_e = \frac{1}{N_A} \sum_j f_j \frac{A_j}{Z_j} \left(\frac{\mu}{\rho}\right)_j \quad \textbf{(4)}$$

Where f_i is fraction by mole of the ith atomic element, A_i is atomic weight of the ith atomic element, Z_j is atomic number and N_A is Avogadro constant.

The effective atomic number which varies with energies can be calculated from the ratio of atomic and electronic cross-sections by the following relation [29-30]:

$$Z_{eff} = \frac{\sigma_a}{\sigma_e} \quad \textbf{(5)}$$

The effective electron number (N_{eff}) is representing the number of electrons per unit mass of the shielding material can be computed using the following relation [29-30]:

$$N_e = \frac{N_A}{A} Z_{eff} \quad \textbf{(6)}$$

Where and A is the mean atomic mass equal to $\sum_i f_i A_i$; f_i is fraction by mole of the ith atomic element, A_i is atomic weight of the ith atomic element

The half-value layer (HVL) and the mean free pass (MFP) are considered as important parameters for the estimation of the required effective shielding thickness for each photon energy. The HVL

is the required thickness to reduce radiation intensity of the mono-energetic beam to its half value, while the MFP is representing the average distance between two successive interaction. These parameters can be computed according to the following relations [29-30]:

$$HVL = \frac{0.693}{\mu} \quad \textbf{(7)}$$

$$MFP = \frac{1}{\mu} \quad \textbf{(8)}$$

Where μ is the linear attenuation coefficient.

4. Results and discussion

Figure 1A and 1B show the computed linear attenuation coefficients (LAC) of the prepared sample ($85TeO_2$-$5Nb_2O_5$-$5ZnO$-$5Ag_2O$) at energy range between 15keV and 1MeV, which correspond to the range of radiographic diagnostic imaging. The LAC for the prepared glass sample were computed using the online developed software (Phy-X/PSD) [24]. The prepared sample recoded the highest values in the energies ranging from 40keV and 90keV as shown in Figure 1A and 1B. For example, the value of linear attenuation coefficient recorded for of the sample was 13.29cm^{-1} compared to 1.148, 6.19, 10.63, 2.11, 2.45, 2.47 and 10.86cm^{-1} at 80keV, with percentage differences of 91.36%, 53.46%, 20%, 84.13% and 81.60%, 81.40% and 18.29 for the common commercial standard materials; RS 253 G18, RS 360, RS 520, Chromite, Chromite, Ferrite, Magnetite and Barite respectively. specified energies range. The superiority of the prepared sample over all standard materials in the diagnostic energy range (40 to 90keV) is due to the fact that Tellurite glass doped with suitable modifier provide more bridging oxygen as host glass network, in addition to thermal stability, durability and good optical properties. These results are consistent with other findings [16, 17, 18].

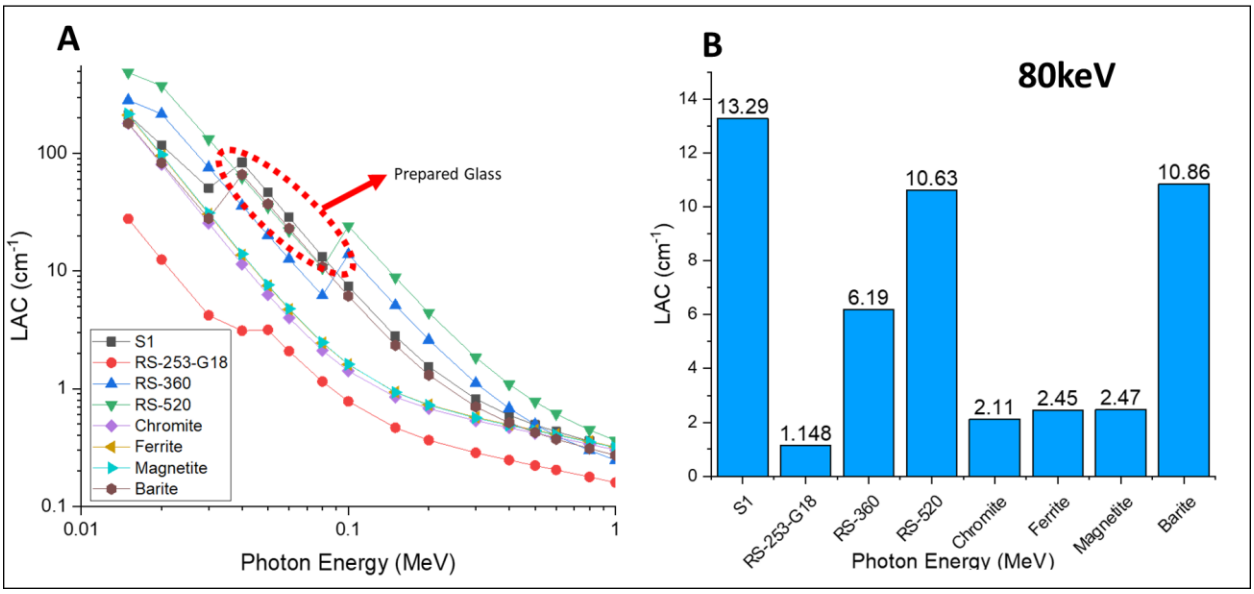

Figure 1. The LAC for proposed glass sample (S1) compared with some common commercial shielding materials; at photon energy range between 15Kev and 1MeV **(A)**; 80keV **(B)**.

Figure 2A and 2B show the computed half-value layers (HVL) of the prepared sample (S1) compared with some commercially available shielding materials such as Schott Co. Germany standard shielding glass materials (RS 253 G18, RS 360, RS 520) [31] and some of the common oxide used with concrete materials such as Chromite, Ferrite, Magnetite and Barite [32], at energy range between 15keV and 1MeV. As shown in the Figure 2A and 2B the recorded HVL values of the sample is lower than the commercially available shielding materials I the energy range between 15keV and 90keV, which is expected due to the higher linear attenuation recorded for sample compared with other samples. For example, the computed MFP value of S1 was found 0.052cm compared to 0.604, 0.056, 0.112, 0.065, 0.329, 0.281 and 0.064cm at 80keV, with percentage differences of 168.3%, 7.4%, 73.1%, 22.2%, 145.4% and 20.7% for the RS 253 G18, RS 360, RS 520, Chromite, Chromite, Ferrite, Magnetite and Barite respectively. The high attenuation recorded is due to the high molecular weight and density of sample 6 compared with the other samples. Above 90keV the prepared glass material shows superior effectiveness over some majority of the commercial materials, while the other standard glasses materials RS-520, RS-360 are slightly better compare with the prepared samples.

As shown in Figure 3A and 3B the prepared sample also recorded the lowest values of MFP compare with the other samples.

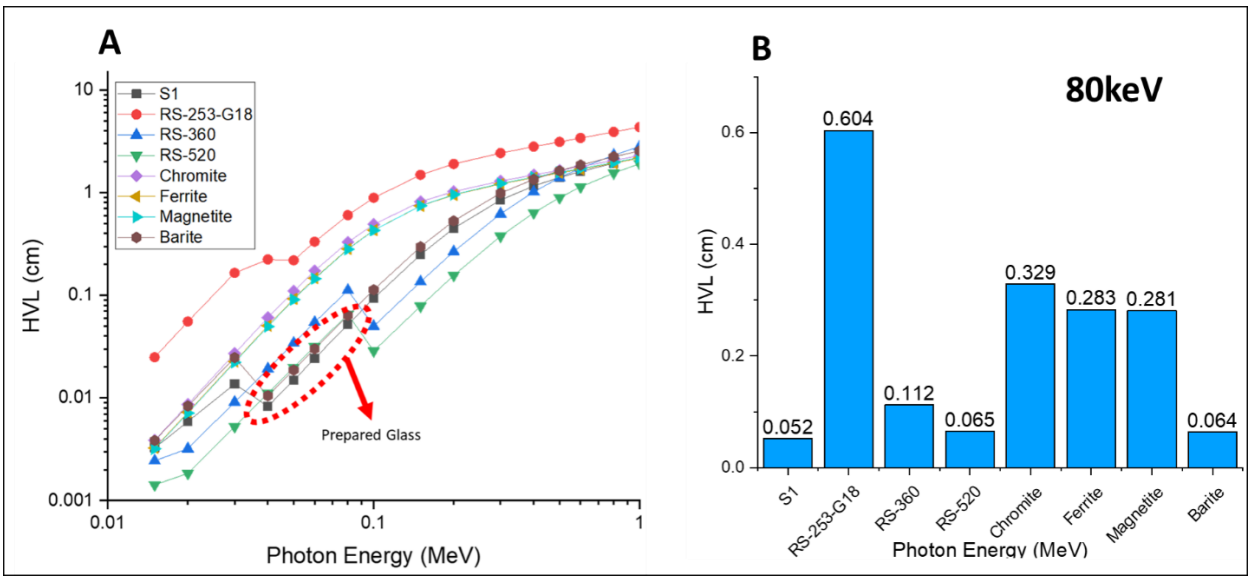

Figure 2 The HVL for proposed glass sample (S1) compared with some common commercial shielding materials; at photon energy range between 15Kev and 1MeV **(A)**; 80keV **(B)**.

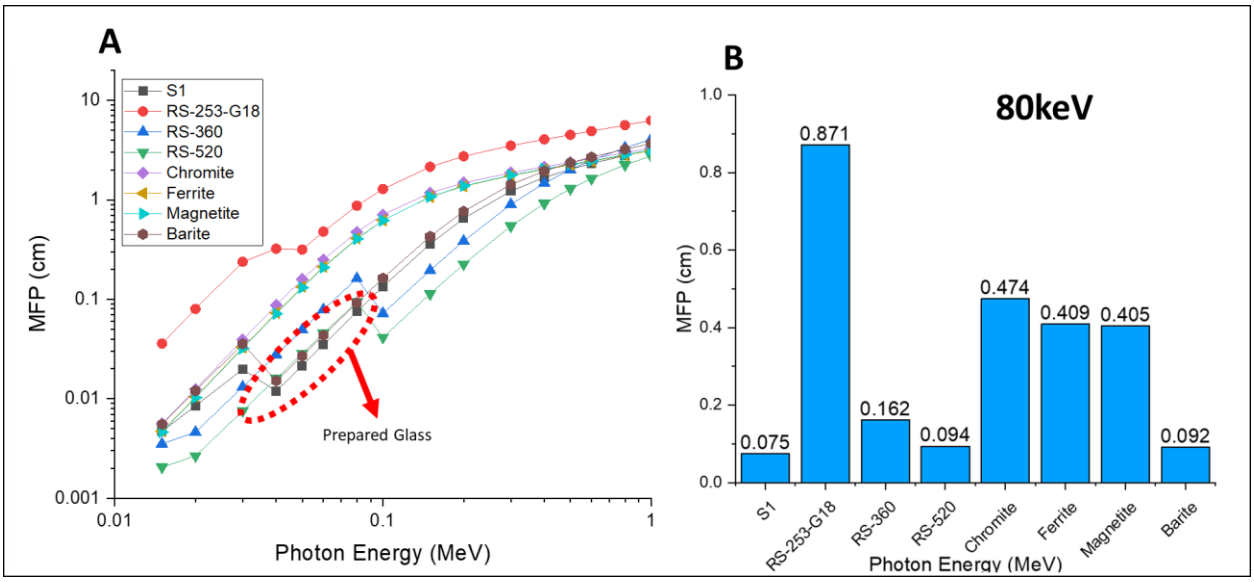

Figure 3. The MFP for proposed glass sample (S1) compared with some common commercial shielding materials; at photon energy range between 15Kev and 1MeV **(A)**; 80keV **(B).**

Figure 4A and 4B shows the values of the total atom cross-section (σ_a) and total electronic cross-section (σ_a) as a function of photon energy for the prepared sample material compared with the commercially available shielding materials. The prepared sample recorded the higher values of $\sigma_a$and σ_a at diagnostic energy range.

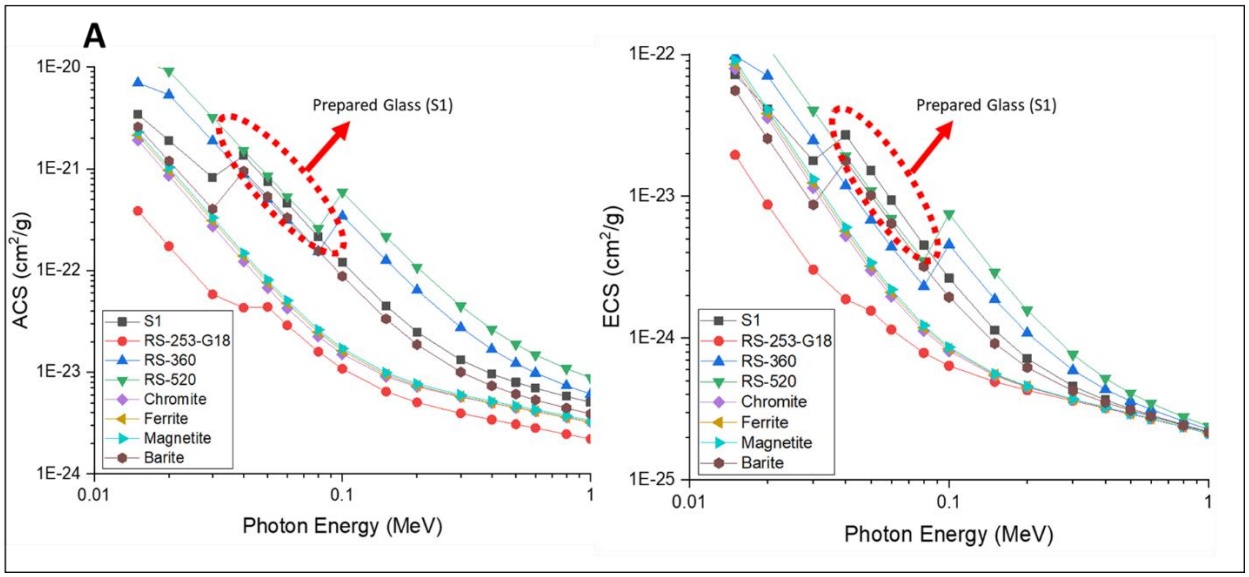

Figure 4. The ACS **(A)** and ECS **(B)** of proposed sample compared with standard materials at photon energy range between 15keV and 1MeV.

Figure 5A and 5B illustrated the effective atomic number (Z_{eff}) and effective electron numbers (N_{eff}) against photon energy (MeV) of the prepared glass sample. The prepared sample recorded comparable values with the commercially available shielding, which consistent with previous findings for linear attenuation coefficient. The maximum Z_{eff} value of 49 was recorded at energy 40keV, while the minimum value of 23.1 is recorded at energy 1MeV, which indicates the better efficiency of the sample as a shielding material compare with the other samples. These results consistent with findings discussed before for linear and mass attenuations.

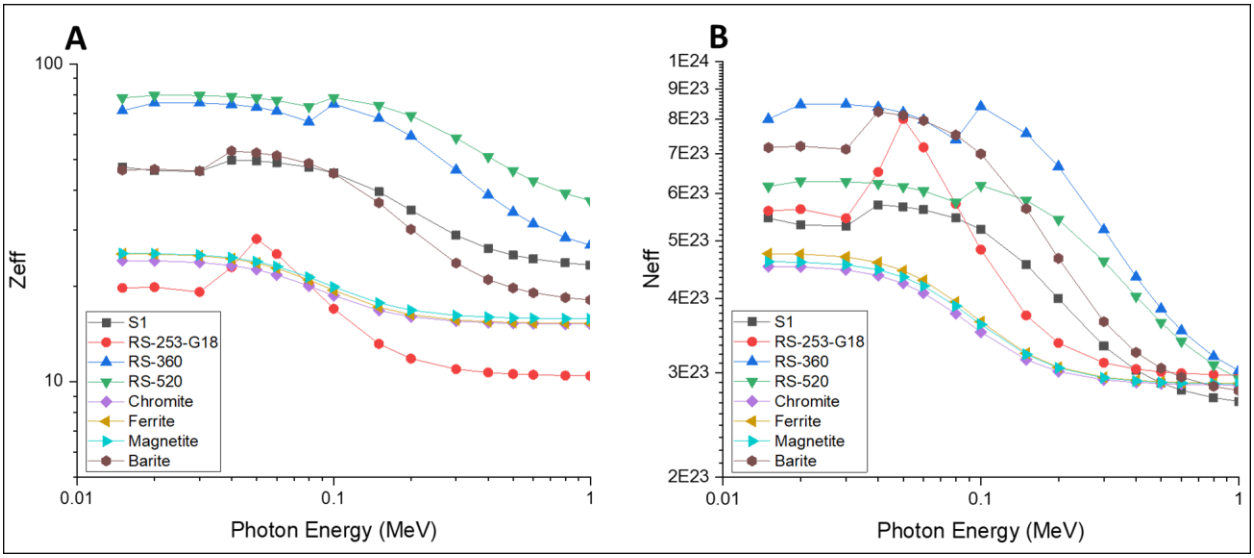

Figure 5. The Z_{eff} **(A)** and the N_{eff} **(B)** of proposed sample compared with standard materials at photon energy range between 15keV and 1MeV.

5. Conclusion

Shielding and physical properties of a tellurite glass sample contain host metal oxides (**$85TeO_2$-$5Nb_2O_5$-5ZnO-$5Ag_2O$**) were evaluated at photon energies range between 15keV and 1MeV. The shielding parameters of the proposed glass system such as linear attenuation coefficients, HVL, MFP, Z_{eff}, and N_{eff} were evaluated. The proposed samples showed a superior performance at the diagnostic energy range between 40 and 90 keV and a comparable shielding effectiveness above 90keV when compared with other commercial standard shielding materials. Each of the metal oxide selected for the preparation of the proposed glass material has its unique properties in term of the good physical and shielding properties such as glass formation, thermal, radiation shielding effectiveness and transparency, which make the prepared sample a promising glass material not only for shielding purposes but also for other medical applications.

3 References

1. Parker HMOD, Joyce MJ. The use of ionizing radiation to image nuclear fuel: A review. Progress in Nuclear Energy. 2015;85:297-318.
2. Vreysen MJB, Robinson AS. Ionising Radiation and Area-Wide Management of Insect Pests to Promote Sustainable Agriculture. 2011:671-92.
3. Smith-Bindman R, Miglioretti DL, Larson EB. Rising use of diagnostic medical imaging in a large integrated health system. *Health Aff (Millwood*). 2008;27(6):1491-502.
4. Johanna M Meulepas, Cécile M Ronckers, Anne M J B Smets, Rutger A J Nievelstein, Patrycja Gradowska, Choonsik Lee, Andreas Jahnen, Marcel van Straten, Marie-Claire Y de Wit, Bernard Zonnenberg, Willemijn M Klein, Johannes H Merks, Otto Visser, Flora E van Leeuwen, Michael Hauptmann. Radiation Exposure From Pediatric CT Scans and Subsequent Cancer Risk in the Netherlands. *JNCI: Journal of the National Cancer Institute*, 2018; DOI: 10.1093/jnci/djy104.
5. Mathews JD, Forsythe AV, Brady Z, et al. Cancer risk in 680,000 people exposed to computed tomography scans in childhood or adolescence: data linkage study of 11 million Australians. BMJ. 2013;346:f2360. Published 2013 May 21. doi:10.1136/bmj.f2360
6. Linet MS, Slovis TL, Miller DL, et al. Cancer risks associated with external radiation from diagnostic imaging procedures [published correction appears in CA Cancer J Clin. 2012 Jul-Aug;62(4):277]. *CA Cancer J Clin.* 2012;62(2):75-100. doi:10.3322/caac.21132
7. Hall EJ, Brenner DJ. Cancer risks from diagnostic radiology: the impact of new epidemiological data. *Br J Radiol*. 2012;**85**(1020):e1316-e1317. doi:10.1259/bjr/13739950
8. Washington: National Academies Press; 2006. Committee to assess health risks from exposure to low levels of ionizing radiation NRC. Health risks from exposure to low levels of ionizing radiation: BEIR VII Phase 2
9. Radiation Protection and Safety in Medical Uses of Ionizing Radiation, IAEA Safety Standards for protecting people and the environment, Specific Safety Guide No. SSG-46. International atomic energy agency (IAEA). Vienna, 2018. Available online at: https://www-pub.iaea.org/MTCD/Publications/PDF/PUB1775_web.pdf

10. International atomic energy agency (IAEA), Justification of Practices, Including Non-medical Human Imaging, IAEA Safety Standards Series No. GSG-5, IAEA, Vienna (2014).
11. International commission on radiation protection. The 2007 Recommendations of the International Commission on Radiological Protection, Publication 103, Elsevier (2007).
12. International atomic energy agency, IAEA Safety Glossary: Terminology Used in Nuclear Safety and Radiation Protection (2007 Edition), IAEA, Vienna (2007).
13. Jamie M. Shoag, Kevin Michael Burns, Sukhraj S. Kahlon, Patrick J. Parsons, Polly E. Bijur, Benjamin H. Taragin & Morri Markowitz (2020) Lead poisoning risk assessment of radiology workers using lead shields, *Archives of Environmental & Occupational Health*, 2020;**75**(1): 60-64, DOI: 10.1080/19338244.2018.1553843.
14. Anink D., Boonstra C., Mak J. (1996). *Handbook of sustainable building*. London: James & James.
15. Balanli A., Ozturk A. Yapinin Ic. Examining indoor and outdoor environments of buildings in terms of building biology. Healthy cities and civil engineering symposium. *Chamber of Turkish Civil Engineers,Izmir Branch*. 1995: 45–55.
16. Helena Ticha, Jiri Schwarz, Ladislav Tichy, Raman spectra and optical band gap in some PbO-ZnO-TeO2 glasses, Mater. Chem. Phys.,2019; 237, 121834.
17. Gedikoğlu N, Ersundu A, Aydin S, Çelikbilek M. Crystallization behavior of WO3-MoO3-TeO2 glasses, J. Non-Cryst. Solids, 2018; 501:93–100.
18. Tekin HO,. Kassab LRP, Ozge Kilicoglu, Evellyn Santos Magalhães, Shams AM, da Silva Mattos GR. Newly developed tellurium oxide glasses for nuclear shielding applications: an extended investigation. J. Non-Cryst. Solids (2019), 10.1016/j.jnoncrysol.2019.11976.
19. Sayyed MI, Kawa MK, Gaikwad DK, Agar O, Gawai UP, Baki SO. Physical, structural, optical and gamma radiation shielding properties of borate glasses containing heavy metals (Bi2O3/MoO3) Journal of Non-Crystalline Solids, 2019;507, pp. 30-37.
20. Chahine A, Et-Tabirou M, Elbenaissi M, Haddad M, Pascal JL. Effect of CuO on the structure and properties of (50–x/2)Na2O-xCuO-(50–x/2)P2O5glasses. *Mater Chem Phys* 2004; **84**:341-347.

21. Al-Hadeethi Y, Sayyed MI, Mohammed H, Rimondin L. X-ray photons attenuation characteristics for two tellurite-based glass systems at dental diagnostic energies. Ceram. Int. 46, 251–257 (2020)
22. Mhareb M., Almessiere M., Sayyed M. I. and Alajerami Y. Physical, structural, optical and photons attenuation attributes of lithium-magnesium-borate glasses: Role of Tm2O3 doping, Optik, 2019;182:821-831.
23. Lakshminarayana G, Sayyed MI, Baki SO, Lira A, Dong M, Kawa M, Kaky M, Kityk I and MahdiOptical MA. Absorption and gamma-radiation-shielding parameter studies of Tm3+-doped multicomponent borosilicate glasses, Applied Physics A, 2018; 124:1-16..
24. Şakar E, Özpolat ÖF, Alım B, Sayyed MI, Kurudirek M. Phy-X/PSD: Development of a user-friendly online software for calculation of parameters relevant to radiation shielding and dosimetry. Radiation Physics and Chemistry. 2020;166:108496-12.
25. Kıbrıslı O, Ersundu AE, Çelikbilek EM. Dy^{3+} doped tellurite glasses for solid-state lighting: An investigation through physical, thermal, structural and optical spectroscopy studies. *Journal of Non-Crystalline Solids* 2019; **513**: 125-136.
26. Hubbell JH, Seltzer SM. Tables of X-Ray Mass Attenuation Coefficients and Mass Energy-Absorption Coefficients 1 keV to 20 MeV for Elements Z=1 to 92 and 48 Additional Substances of Dosimetric Interest. National Institute of Standards and Technology 1995 - PL, Gaithersburg, USA
27. Hubbell JH. Review of photon interaction cross section data in the medical and biological context. Phys. Med. Biol 1999; 44: R1-R22.
28. Gerward L, Guilbert N, Jensen KB, Levring H. WinXCom - a program for calculating X-ray attenuation coefficients. Radiat. Phys. Chem 2004; 71: 653-654
29. Taylor ML, Smith RL, Dossing F, Franich RD. Robust calculation of effective atomic numbers: the Auto-Z(eff) software. Med. Phys. 2012; 39:1769-1778.
30. Un at, Caner T. The Direct-Z(eff) software for direct calculation of mass attenuation coefficient, effective atomic number and effective electron number. Ann. Nucl. Energy 2014; 65:158-165.
31. Schott Co:
URL: https://www.schott.com/advanced_optics/english/products/optical-materials/special-materials/radiation-shielding-glasses/index.html

32. Kaundal RS. Comparative Study of Radiation Shielding Parameters for Bismuth Borate Glasses. *Materials Research* 2016;**19**(4):776-78